# Measuring the Influence of the $BK_{Ca}$ β1 Subunit on $Ca^{2+}$ Binding to the $BK_{Ca}$ Channel

Tara-Beth Sweet and Daniel H. Cox

Molecular Cardiology Research Institute, Tufts Medical Center, and The Department of Neuroscience, Tufts University School of Medicine, Boston, MA 02111

The large-conductance $Ca^{2+}$-activated potassium ($BK_{Ca}$) channel of smooth muscle is unusually sensitive to $Ca^{2+}$ as compared with the $BK_{Ca}$ channels of brain and skeletal muscle. This is due to the tissue-specific expression of the $BK_{Ca}$ auxiliary subunit β1, whose presence dramatically increases both the potency and efficacy of $Ca^{2+}$ in promoting channel opening. β1 contains no $Ca^{2+}$ binding sites of its own, and thus the mechanism by which it increases the $BK_{Ca}$ channel's $Ca^{2+}$ sensitivity has been of some interest. Previously, we demonstrated that β1 stabilizes voltage sensor activation, such that activation occurs at more negative voltages with β1 present. This decreases the work that $Ca^{2+}$ must do to open the channel and thereby increases the channel's apparent $Ca^{2+}$ affinity without altering the real affinities of the channel's $Ca^{2+}$ binding sites. To explain the full effect of β1 on the channel's $Ca^{2+}$ sensitivity, however, we also proposed that there must be effects of β1 on $Ca^{2+}$ binding. Here, to test this hypothesis, we have used high-resolution $Ca^{2+}$ dose–response curves together with binding site–specific mutations to measure the effects of β1 on $Ca^{2+}$ binding. We find that coexpression of β1 alters $Ca^{2+}$ binding at both of the $BK_{Ca}$ channel's two types of high-affinity $Ca^{2+}$ binding sites, primarily increasing the affinity of the RCK1 sites when the channel is open and decreasing the affinity of the $Ca^{2+}$ bowl sites when the channel is closed. Both of these modifications increase the difference in affinity between open and closed, such that $Ca^{2+}$ binding at either site has a larger effect on channel opening when β1 is present.

The Journal of General Physiology

## INTRODUCTION

Large-conductance $Ca^{2+}$-activated potassium ($BK_{Ca}$) channels are crucial for the regulation of arterial tone, where they facilitate a negative feedback mechanism that opposes vasoconstriction (Nelson et al., 1995; Nelson and Quayle, 1995; Brenner et al., 2000). Intravascular pressure increases arterial tone by a complex process that includes membrane depolarization and the subsequent elevation of cytoplasmic $Ca^{2+}$ via voltage-dependent $Ca^{2+}$ channels. This global increase in $Ca^{2+}$ leads to vasoconstriction, but it also triggers localized $Ca^{2+}$ release events from ryanodine receptors on the smooth muscle sacroplasmic reticulum. These release events, termed $Ca^{2+}$ sparks, activate nearby $BK_{Ca}$ channels that then create a hyperpolarizing $K^+$ current known as a STOC. STOCs then oppose further constriction (Nelson et al., 1995; Perez et al., 1999). The $BK_{Ca}$ channel's accessory β1 subunit has been show to be critically important in this regulatory process, as mice that lack β1 have greatly reduced STOCs in response to sparks as well as hypercontractile smooth muscle and hypertension (Brenner et al., 2000; Pluger et al., 2000). In heterologous expression systems β1 subunits, four of which assemble with a single channel (Shen et al., 1994), make the $BK_{Ca}$ channel substantially more $Ca^{2+}$ sensitive (McManus et al., 1995; Meera et al., 1996; Cox and Aldrich, 2000a). Thus, in the absence of β1 it appears that $BK_{Ca}$ channels lack the $Ca^{2+}$ sensitivity required for $BK_{Ca}$-mediated feedback regulation of smooth muscle tone.

The mechanism by which β1 enhances the $BK_{Ca}$ channel's $Ca^{2+}$ sensitivity has been the subject of many studies (Wallner et al., 1996; Nimigean and Magleby, 1999b, 2000; Cox and Aldrich, 2000b; Qian et al., 2002; Qian and Magleby, 2003; Bao and Cox, 2005; Orio and Latorre, 2005; Morrow et al., 2006; Orio et al., 2006; Wang and Brenner, 2006; Yang et al., 2008), but it is still unclear. Nimigean and Magleby (1999a,b, 2000) found that β1 increases the length of time that the $BK_{Ca}$ channel spends in bursting states and that this effect persists in the absence of $Ca^{2+}$ (Nimigean and Magleby, 1999a). They suggested that a $Ca^{2+}$-independent effect underlies most of the channel's increased $Ca^{2+}$ sensitivity. In support of this notion, Bao and Cox (2005) found, when studying gating currents, that β1 stabilizes voltage sensor activation such that activation occurs at more negative voltages with β1 present. At most voltages this decreases the work that $Ca^{2+}$ must do to open the channel and thereby increases the channel's apparent $Ca^{2+}$

Correspondence to Daniel H. Cox: dan.cox@tufts.edu

Abbreviations used in this paper: $BK_{Ca}$, large-conductance $Ca^{2+}$-activated potassium; G-V, conductance–voltage; HA, Horrigan and Aldrich; *Popen*, open probability.



The Rockefeller University Press $30.00
J. Gen. Physiol. Vol. 133 No. 2 139–150
www.jgp.org/cgi/doi/10.1085/jgp.200810129

affinity. However, to account for the full change in $Ca^{2+}$ sensitivity brought about by β1, Bao and Cox (2005) also proposed that β1 alters the true affinities of the channel's high-affinity $Ca^{2+}$ binding sites (Bao et al., 2004), a conclusion supported by the earlier study of Cox and Aldrich (2000).

A recent paper by Yang et al. (2008), however, suggests that this may not be the case. Their experiments revealed that mutation of the voltage sensor residue R167 eliminates the ability of β1 to enhance the $BK_{Ca}$ channel's $Ca^{2+}$ sensitivity, implying that β1 enhances $Ca^{2+}$ sensitivity solely by altering the conformation or movements of the voltage sensor. Here, to clarify this issue, we have used high-resolution $Ca^{2+}$ dose–response curves to determine directly whether or not β1 alters the $BK_{Ca}$ channel's affinity for $Ca^{2+}$ at either of its two types of high-affinity $Ca^{2+}$ binding sites. We find effects of β1 on the real affinities of both sites.

## MATERIALS AND METHODS

### Heterologous Expression of $BK_{Ca}$ Channels in TSA 201 Cells

TSA 201 cells (modified human embryonic kidney cells) were transiently transfected with expression vectors (pcDNA 3; Invitrogen) encoding the mouse α subunit (mslo-mbr5) (Butler et al., 1993), the mouse β1 subunit of the $BK_{Ca}$ channel, enhanced green fluorescent protein (eGFP-N1; BD), and the empty pcDNA 3.1+ vector (Invitrogen) to control for the total amount of transfected DNA. Cells were transiently transfected using the Lipofectamine 2000 reagent (Invitrogen). The eGFP was used to monitor successfully transfected cells. For transfection, cells at 80–90% confluence in 35-mm falcon dishes were incubated with a mixture of the plasmids (total of 4 μg DNA) Lipofectamine and Optimem (Invitrogen) according to the manufacturer's instructions. In brief, the mixture was left on the cells 4–8 h after which the cells were replated into recording Falcon 3004 dishes in standard tissue culture media: DMEM with 1% fetal bovine serum, 1% L-glutamine, and 1% penicillin-streptomycin solution (all from Invitrogen). The cells were patch clamped 1–3 d after transfection.

The molar ratio of β1 to α-expressing plasmids transfected was 1 β1 plasmid to between 0.6 and 2 α plasmids for all experiments. These ratios were determined to be well above that required to maximize the effects of β1 on channel gating in experiments in which the relative amount of β1 to α plasmid was titrated until no further effect of β1 was observed. The minimal saturating ratio was determined to be 1 β1 plasmid to 6.8 α plasmids, as determined by the magnitudes of β1-induced G-V shifts at 100 μM $[Ca^{2+}]$. This is likely due to more efficient transcription and or translation of β1 relative to the much larger α subunit.

### Electrophysiology

All recordings were done in the inside-out patch clamp configuration (Hamill et al., 1981). Patch pipettes were made of borosilicate glass (VWR micropipettes) with 0.8–5-MΩ resistances that were varied for different recording purposes. The tips of the patch pipettes were coated with sticky wax (KerrLab) and fire polished. Data were acquired using an Axopatch 200B patch clamp amplifier and a Macintosh-based computer system equipped with an ITC-16 hardware interface and Pulse acquisition software (HEKA). For macroscopic current recordings, data were sampled at 50 kHz and filtered at 10 kHz. In most macroscopic current recordings, capacity and leak current were subtracted using a P/5 subtraction protocol with a holding potential of −120 mV and leak pulses in opposite polarity to the test pulse, but with $BK_{Ca}$ currents recorded with >100 μM $Ca^{2+}$, no leak subtraction was performed. Unitary–current recordings acquired at 0 mV were sampled at 100 kHz and filtered at 2 kHz. All experiments were performed at room temperature, 22–24°C.

### Solutions

The pipette solution for macroscopic current recordings contained the following (in mM): 118 $KMeSO_3$, 20 *N*-methyl-glucamine-$MeSO_3$, 2 KCl, 2 $MgCl_2$, and 2 HEPES, pH 7.20. The pipette solution for current recordings at 0 mV contained the following (in mM): 3 $KMeSO_3$, 135 *N*-methyl-glucamine-$MeSO_4$, 2 KCl, 2 $MgCl_2$, and 2 HEPES, pH 7.20. 10 μM $GdCl_3$ was added to both pipette solutions to block endogenous stretch-activated channels (Yang and Sachs, 1989; Qian and Magleby, 2003). The bath solution for all recordings contained the following (in mM): 118 $KMeSO_3$, 20 *N*-methyl-glucamine-$MeSO_3$, 2 KCl, and 2 HEPES, pH 7.20. 1 mM EGTA (Fluka) was used as the $Ca^{2+}$ buffer for solutions containing 3–500 nM free $[Ca^{2+}]$, 1 mM HEDTA (Sigma-Aldrich) was used as the $Ca^{2+}$ buffer for solutions containing 0.8–20 μM free $[Ca^{2+}]$, and no $Ca^{2+}$ chelator was used as the $Ca^{2+}$ buffer in solutions containing between 20 μM and 2.5 mM free $Ca^{2+}$. 50 μM (+)-18-crown-6-tetracarboxylic acid (18C6TA) was added to all internal solutions to prevent contaminant $Ba^{2+}$ block at high voltages. Both internal and external solutions were brought to pH 7.20.

The appropriate amount of total $Ca^{2+}$ (100 mM $CaCl_2$ standard solution; Orion Research, Inc.) to add to the buffered solutions to yield the desired approximate free $Ca^{2+}$ concentrations of 3 nM to 2.5 mM was calculated using the program MaxChelator (see Online supplemental material below), and the solutions were prepared as described previously (Bao et al., 2002). The $Ca^{2+}$ concentrations reported above were determined with an Orion $Ca^{2+}$-sensitive electrode. The solutions bathing the intracellular side of the patch were changed by means of a DAD valve controlled pressurized superfusion system (ALA Scientific Instruments).

### Data Analysis

All data analysis was performed with Igor Pro graphing and curve-fitting software (WaveMetrics, Inc.), and the Levenberg-Marquardt algorithm was used to perform nonlinear least-square curve fitting. Values in the text are given ± the standard error of the mean.

### Conductance–Voltage (G-V) Curves

G-V relations were determined from the amplitude of tail currents measured 200 μs after repolarizations to −80 mV following voltage steps to the test voltage. Each G-V relation was fitted with a Boltzmann function,

$$G = G_{\max} / [1 + e^{\frac{-zF(V - V_{1/2})}{RT}}],$$

and normalized to the maximum of the fit.

### Single-channel Analysis

Under conditions where the open probability (*Popen*) is small ($<10^{-2}$), single-channel openings were observed in patches containing hundreds of channels and $I_K$ was measured from steady-state recordings 30 s in duration. *NPopen* was determined from all-points histograms by measuring the fraction of time spent ($P_K$) at each open level (*k*) using a half-amplitude criteria and summing their contributions $NPopen = \Sigma\ kP_K$, where *N* is the number of channels in the patch.

### *Popen* versus $Ca^{2+}$ Curves

The effect of $Ca^{2+}$ on *Popen* was determined from the ratio of *NPopen* at a given [$Ca^{2+}$] to *NPopen* at 0.88 or 5.4 µM $Ca^{2+}$ for all [$Ca^{2+}$] tested on a given patch. In the presence of β1, the range of total activity per patch obtained over the range of [$Ca^{2+}$] tested (3 nM to 2.5 mM) was greater than could be covered with a single normalization point. Therefore, in patches with many channels from which we were most interested in making low *Popen* measurements, the *NPopen* data at each [$Ca^{2+}$] was normalized by the *NPopen* value measured at 0.88 µM [$Ca^{2+}$]. Such curves were then averaged. Likewise, in patches with fewer channels, from which we were most interested in making higher *Popen* measurements, the *NPopen* data at each [$Ca^{2+}$] was normalized by the *NPopen* value measured at 5.4 µM [$Ca^{2+}$], and these curves were then averaged. The curve normalized to 0.88 µM was then adjusted so as to have the same value at 0.88 µM [$Ca^{2+}$] as the curve normalized to 5.4 µM [$Ca^{2+}$]. To yield a single curve at the [$Ca^{2+}$] at which the two curves overlapped, the two values present were subjected to a weighted average, weighted by the number of measurements in each of the two curves being brought together. This yielded a $Ca^{2+}$ dose–response curve with a value of 1 at 5.4 µM. This curve was then rescaled vertically so that the bottom of the curve equaled 1, or 0 on a log scale. This final curve we plotted as ($NPopen/NPopen_{min}$).

In some cases, *Popen* rather than ($NPopen/NPopen_{min}$) was reported as a function of [$Ca^{2+}$]. This was done by determining *Popen* for each channel type at a single [$Ca^{2+}$] in separate experiments, and then adjusting the average log ($NPopen/NPopen_{min}$) versus log [$Ca^{2+}$] curve vertically, such that *Popen* was correct at the [$Ca^{2+}$] at which *Popen* was known. This *Popen*, used for calibration, was determined at 2.5 mM [$Ca^{2+}$] from patches whose channel content was apparent ($n$ = 1–4).

### Online Supplemental Material

The amount of $Ca^{2+}$ to add to internal solutions to yield the desired free $Ca^{2+}$ concentrations was calculated using the program MaxChelator, which was downloaded from http://www.stanford.edu/~cpatton/maxc.html and is included as executable files available at http://www.jgp.org/cgi/content/full/jgp.200810094/DC1.

## RESULTS

### Steady-state Effects of β1

The $BK_{Ca}$ channel is both $Ca^{2+}$ and voltage sensitive, and the effects of these stimuli are often displayed as a series of G-V relations determined over a series of $Ca^{2+}$ concentrations. Such a series, determined from current families recorded from $BK_{Ca}$ channels expressed in TSA 201 cells, is shown in Fig. 1 C. Representative data used to construct such a series are shown in Fig. 1 A. The data are from an excised inside-out macropatch expressing the mouse $BK_{Ca}$ α subunit (mSlo1). Increasing intracellular $Ca^{2+}$ shifts the channels' G-V curve leftward, an effect that is generally known to be due to three types of $Ca^{2+}$ binding sites, two of high affinity and one of low affinity (Schreiber and Salkoff, 1997; Bian et al., 2001; Bao et al., 2002, 2004; Shi et al., 2002; Xia et al., 2002). The channels in these patches, however, contained the mutation E399N, which eliminates low-affinity $Ca^{2+}$ sensing (Shi et al., 2002; Xia et al., 2002). So here only the effects of $Ca^{2+}$ binding at the channel's high-affinity $Ca^{2+}$ binding sites are evident. We refer to the mSlo1 channel carrying this mutation as ΔE. Increasing $Ca^{2+}$ from 3 nM to 2.5 mM shifts the ΔE G-V relation ∼200 mV leftward.

When the mouse $BK_{Ca}$ β1 subunit is expressed with the α subunit (see currents in Fig. 1 B), the $Ca^{2+}$-induced leftward shifting evident in Fig. 1 C becomes more pronounced (Fig. 1 D), and thus it may be said that β1 increases the $Ca^{2+}$ sensitivity of the $BK_{Ca}$ channel in that it increases its G-V shift in response to a given change in [$Ca^{2+}$] (McManus et al., 1995). On a plot of half-maximal activation voltage ($V_{1/2}$) versus [$Ca^{2+}$], this effect is seen as an increase in slope (Fig. 1 E). At a single membrane voltage, 0 mV for example, it appears as an increase in both the efficacy and the apparent affinity of the channel for $Ca^{2+}$ (Fig. 1 F). These data reveal that $Ca^{2+}$ binding to the $BK_{Ca}$ channel's low-affinity $Ca^{2+}$ binding sites (eliminated by the E399N mutation) is not required for β1's effects on $Ca^{2+}$ sensing. β1 has similar effects on the ΔE channel as it does on wild-type mSlo1 (McManus et al., 1995; Cox and Aldrich, 2000a; Bao and Cox, 2005).

### Estimating the Affinities of Each Binding Site with and without β1

In a previous study we found that much of β1's effects on $Ca^{2+}$ sensing are due to its effects on voltage sensor movement, but to completely account for our data, we suggested that β1 also has effects on $Ca^{2+}$ binding (Bao and Cox, 2005). Here, to test this hypothesis we sought to estimate the channel's $Ca^{2+}$ dissociation constants at each high-affinity $Ca^{2+}$ binding site in the presence and absence of β1. To do this we used high-resolution $Ca^{2+}$ dose–response curves (Horrigan and Aldrich, 2002; Sweet and Cox, 2008). The channel's *Popen* was measured at a single voltage over a large range of [$Ca^{2+}$]. Fig. 2 (A and B) shows unitary currents recorded from membrane patches expressing either ΔE or ΔE + β1. Both patches were held at 0 mV and exposed to a range of [$Ca^{2+}$]. Although each patch contained many channels, *Popen* was low at 3 nM [$Ca^{2+}$], such that activity was observed as the infrequent and brief openings of single channels. Increasing intracellular $Ca^{2+}$ then caused an increase in *Popen*. From data like these we derived the ΔE and ΔE + β1 channels' *Popen* versus [$Ca^{2+}$] relations (Fig. 2 C). So that all parts of each curve could be well determined, *Popen* was measured over seven orders of magnitude with 21 $Ca^{2+}$ concentrations. To do this, many patches were used and normalized by their values of *NPopen* at 5.3 µM, where $N$ is the number of channels in a given patch. The resulting curve was then either normalized to its minimum to yield curves like those in Fig. 3 C or adjusted so as to have the proper *Popen* at 2.5 mM [$Ca^{2+}$] (determined in separate single-channel experiments; see Materials and methods). This yielded curves like those in Fig. 2 D.

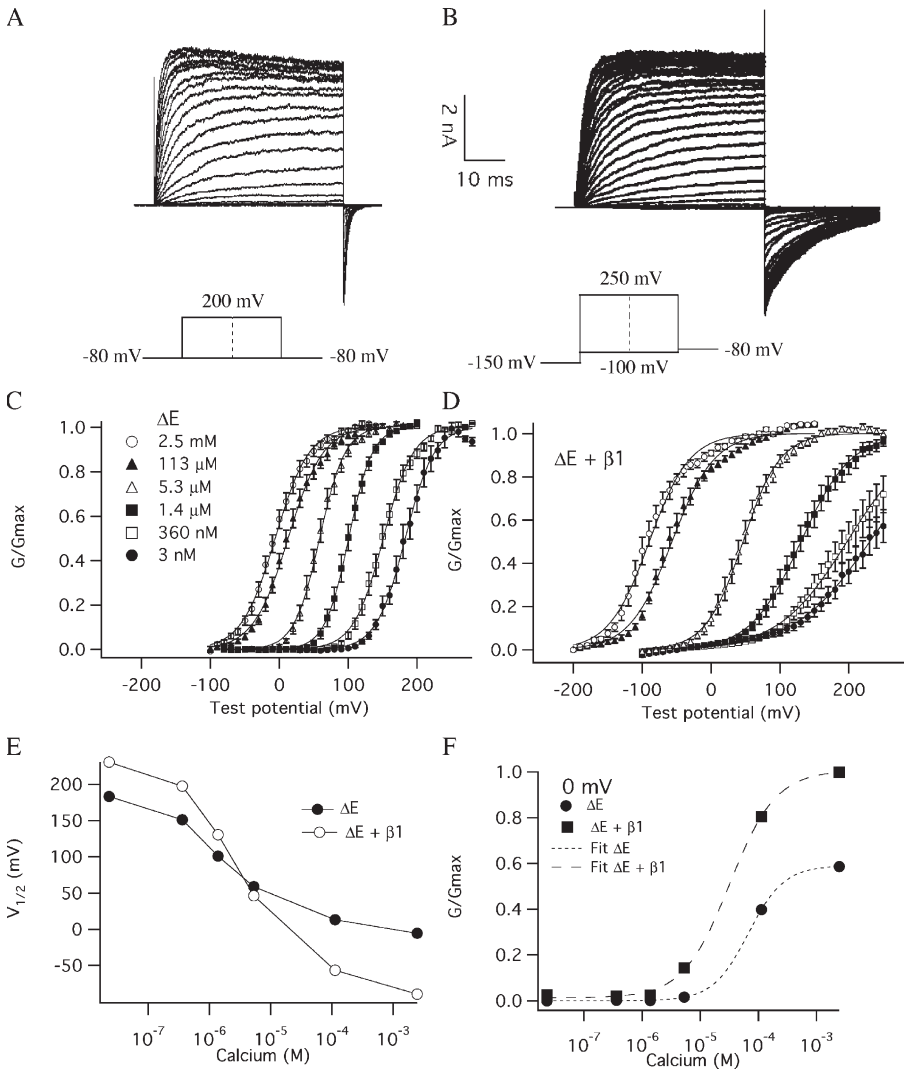


**Figure 1.** β1 increases the $Ca^{2+}$ sensitivity of $BK_{Ca}$-channel activation. (A and B) Macroscopic currents recorded from ΔE channels in the absence and presence of β1. Currents are from inside-out macropatches from TSA 201 cells exposed to 9.7 μM $Ca^{2+}$. (C and D) G-V relations determined at the following $Ca^{2+}$ concentrations: 0.003, 0.360, 1.4, 5.3, 113, and 2,500 μM for the mutant channel ΔE (C) and ΔE + β1 (D). Each curve represents the average of between 4 and 22 individual curves. Error bars indicate SEM. The solid curves are Boltzmann fits with the following parameters: ΔE, 3 nM $Ca^{2+}$: Q = 1.21 *e*, $V_{1/2}$ = 183 mV; 360 nM $Ca^{2+}$: Q = 1.18 *e*, $V_{1/2}$ = 151 mV; 1.4 μM $Ca^{2+}$: Q = 1.47 *e*, $V_{1/2}$ = 101 mV; 5.4 μM $Ca^{2+}$: Q = 1.38 *e*, $V_{1/2}$ = 59 mV; 113 μM $Ca^{2+}$: Q = 1.00 *e*, $V_{1/2}$ = 13 mV; 2.5 mM $Ca^{2+}$: Q = 1.04 *e*, $V_{1/2}$ = −5.7 mV. ΔE + β1, 3 nM $Ca^{2+}$: Q = 0.46 *e*, $V_{1/2}$ = 230 mV; 360 nM $Ca^{2+}$: Q = 0.51 *e*, $V_{1/2}$ = 197 mV; 1.4 μM $Ca^{2+}$: Q = 0.70 *e*, $V_{1/2}$ = 131 mV; 5.4 μM $Ca^{2+}$: Q = 0.94 *e*, $V_{1/2}$ = 46 mV; 113 μM $Ca^{2+}$: Q = 0.83 *e*, $V_{1/2}$ = −57 mV; 2.5 mM $Ca^{2+}$: Q = 0.87 *e*, $V_{1/2}$ = −90 mV. (E) Plots of half-maximal activation voltage ($V_{1/2}$) versus [$Ca^{2+}$] for traces shown in C and D. (F) $Ca^{2+}$ dose–response curves determined for ΔE in the presence and absence of β1 at 0 mV. The curves are fitted with the Hill equation:

$$\frac{G}{G_{\max}} = \frac{1}{1+(Kd/[Ca])^n}.$$

Fit parameters are as follows: ΔE (Kd = 68 μM, *n* = 1.4); ΔE + β1 (Kd = 32 μM, *n* = 1.1).

Fig. 2 C shows a comparison of the $Popen/Popen_{min}$ versus [$Ca^{2+}$] relations at 0 mV of the ΔE channel in the presence (filled circles) and absence (open circles) of β1. The magnitude of the change in *Popen* induced by $Ca^{2+}$ (the range the data spans on the ordinate) is ∼100-fold larger for the ΔE + β1 channel than it is for the ΔE channel. This magnitude is determined by the energy $Ca^{2+}$ binding imparts to the channel's central closed-to-open conformational change, which in turn is determined by the open- and closed-state $Ca^{2+}$ binding affinities of each binding site. Thus, that this magnitude changes with β1 coexpression indicates that β1 alters $Ca^{2+}$ binding.

To analyze this effect more rigorously, *Popen* versus [$Ca^{2+}$] relations were determined for the ΔE (open circles) and ΔE + β1 (filled circles) channels (Fig. 2 D), and these data were then analyzed as follows. If one assumes that there are four of each type of $Ca^{2+}$ binding site and that each site influences channel opening by altering the equilibrium constant of a single conformational change between closed and open—as much evidence suggests (McManus and Magleby, 1991; Cox et al., 1997; Cui et al., 1997; Horrigan et al., 1999; Horrigan and Aldrich, 1999, 2002; Rothberg and Magleby, 1999, 2000; Cox and Aldrich, 2000a)—and that there are no interactions between binding sites and no interactions between binding sites and voltage sensors (not rigorously true [Sweet and Cox, 2008], but see below), then at constant voltage the channel's *Popen* as a function of voltage can be written as

$$Popen = \frac{M(1+[Ca]/K_{O1})^4(1+[Ca]/K_{O2})^4}{(1+[Ca]/K_{C1})^4(1+[Ca]/K_{C2})^4 + M(1+[Ca]/K_{O1})^4(1+[Ca]/K_{O2})^4}, \quad (1)$$

where $K_{C1}$ and $K_{C2}$ represent the dissociation constants of binding sites 1 and 2 in the closed conformation, $K_{O1}$ and $K_{O2}$ represent the dissociation constants of binding sites 1 and 2 in the open conformation, and *M* represents the closed-to-open equilibrium constant when no $Ca^{2+}$ are bound. As relates to the $BK_{Ca}$ channel, *M* is voltage dependent and incorporates all effects of voltage on opening.

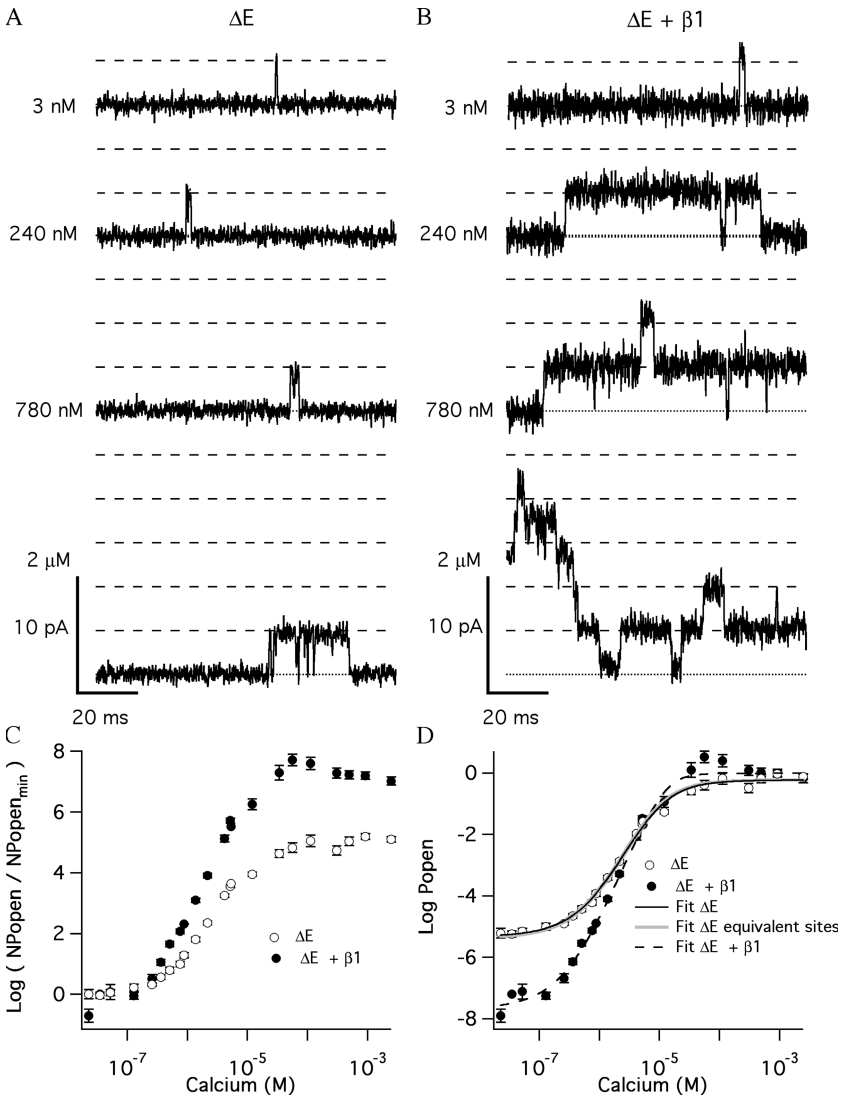


**Figure 2.** β1 increases the $Ca^{2+}$ dependence of *Popen* at a constant voltage. (A and B) Outward $K^+$ currents recorded at 0 mV and filtered at 2 kHz from macropatches containing ΔE channels (A) or ΔE + β1 channels (B) exposed to the indicated [$Ca^{2+}$]. These currents demonstrate that *Popen* increases in a $Ca^{2+}$-dependent manner when voltage is constant. A comparison of the dose–response relations for the effect of $Ca^{2+}$ on *Popen* at 0 mV in the absence or presence of β1 is show. Each point represents the average of between 7 and 30 patches at each [$Ca^{2+}$] tested. Error bars represent SEM. The *Popen* curves are fitted with Eq. 1 yielding values of: ΔE, $K_{C1} = 4.3$ μM, $K_{O1} = 1.1$ μM, $K_{C2} = 7.9$ μM, $K_{O2} = 1.3$ μM, $M = 4.7 \times 10^{-6}$; ΔE + β1, $K_{C1} = 2.2$ μM, $K_{O1} = 0.5$ μM, $K_{C2} = 32$ μM, $K_{O2} = 0.6$ μM, $M = 2.0 \times 10^{-8}$. Additionally, ΔE was fitted assuming that the two types of binding sites are equivalent. The fit yield values of $K_C = 5.9$ μM, $K_O = 1.2$ μM, and $M = 4.2 \times 10^{-6}$.

In the absence of $Ca^{2+}$, Eq. 1 reduces to:

$$Popen = \frac{M}{1+M}, \tag{2}$$

which can be rearranged to

$$M = \frac{Popen}{1-Popen}. \tag{3}$$

Further, at voltages where Popen is much less than 1 ($\sim 10^{-2}$ or lower, such as 0 mV, which we have used here), Eq. 3 may be simplified to

$$M \approx Popen. \tag{4}$$

Thus, in the absence of $Ca^{2+}$, *M* can be determined directly from *Popen*.

Conversely, at saturating $Ca^{2+}$, Eq. 1 reduces to

$$Popen = \frac{1}{1+\frac{1}{M}\left(\frac{1}{C1}\right)^4\left(\frac{1}{C2}\right)^4} \tag{5},$$

where

$$C1 = \left(\frac{K_{C1}}{K_{O1}}\right) \tag{6},$$

and

$$C2 = \left(\frac{K_{C2}}{K_{O2}}\right) \tag{7}$$

and, therefore, the top of the *Popen* versus [$Ca^{2+}$] curve is determined by *M* and the ratios (*C1* and *C2*) of the open- and closed-state $Ca^{2+}$ dissociation constants at the two types of sites.

The ΔE channel's *Popen* versus [$Ca^{2+}$] curve at 0 mV (Fig. 2 D, open circles) was fitted with Eq. 1 (solid line). The fit yielded the following values:

Site 1: $K_{C1} = 4.3 \pm 21$ μM, $K_{O1} = 1.1 \pm 19$ μM, C = 3.9
Site 2: $K_{C2} = 7.9 \pm 20$ μM, $K_{O2} = 1.3 \pm 24$ μM, C = 6.1
$M = 4.7 \times 10^{-6} \pm 10^{-6}$

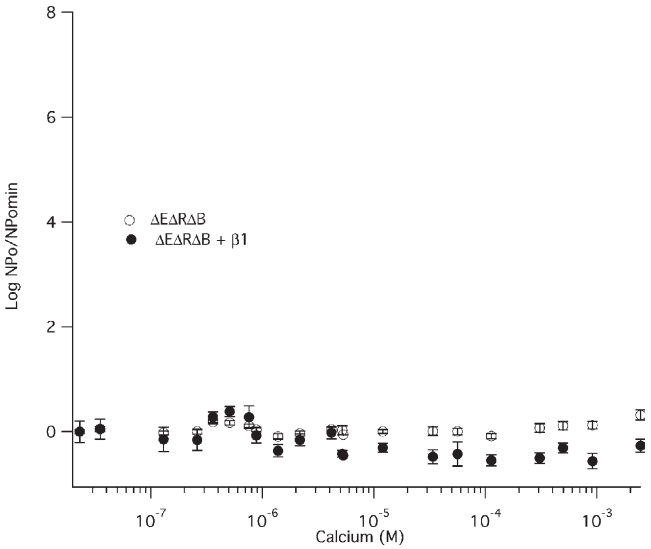


**Figure 3.** Mutating all three types of $Ca^{2+}$ binding sites eliminates the $Ca^{2+}$ dependence of *Popen*. Dose–response relationships for the effect of $Ca^{2+}$ on *Popen* at 0 mV were obtained by plotting the mean log ratio of N*Popen* in the presence and absence of $Ca^{2+}$ for ΔEΔRΔB (open circles) and ΔEΔRΔB + β1 (filled circles) channels. Each point represents the average between 7 and 11 patches at each [$Ca^{2+}$] tested. Error bars represent SEM.

Note the large standard errors of the dissociation constants. This suggests that the fit is not unique and that the RCK1 and $Ca^{2+}$ bowl sites likely have similar affinities at 0 mV, such that changes in the parameters governing one site can be compensated for by changes in the parameters governing the other site. Indeed, the fit was almost as good when we supposed that the two types of sites had identical binding properties (gray curve).

Also shown in Fig. 2 D is the *Popen* versus [$Ca^{2+}$] curve we determined for the ΔE channel in the presence of β1. β1 reduces *M* by 235-fold, which moves the 0 [$Ca^{2+}$] data point well down the ordinate. This indicates that some of β1's effects are on channel properties that are unrelated to $Ca^{2+}$ binding, as has been demonstrated (Nimigean and Magleby, 1999b, 2000; Bao and Cox, 2005; Orio and Latorre, 2005; Wang and Brenner, 2006). Fitting this curve with Eq. 1 yielded:

$$\text{Site 1: } K_{C1} = 2.2 \pm 0.3\ \mu M,\ K_{O1} = 0.50 \pm 2.1\ \mu M,\ C = 4.4$$
$$\text{Site 2: } K_{C2} = 32 \pm 0.0\ \mu M,\ K_{O2} = 0.56 \pm 1.9\ \mu M,\ C = 57.1$$
$$M = 2.0 \times 10^{-8} \pm 21 \times 10^{-6}$$

The fit is better determined than the fit to the ΔE (α only) curve, and it suggests that in addition to decreasing *M* ~200-fold, β1 increases the affinity of both binding sites when the channel is open, and it reduces the affinity of one site when the channel is closed. This increases *C* at both sites and thereby the effect of $Ca^{2+}$ binding on channel opening.

### β1 Does not Restore $Ca^{2+}$ Sensing to Triple Mutant Channels

To test more directly whether β1 affects $Ca^{2+}$ binding, and if so, at which sites and to what extent, we examined β1's effects on each type of binding site individually using mutations that selectively eliminate the effect of $Ca^{2+}$ at each type of site. D367A eliminates $Ca^{2+}$ sensing via RCK1 sites (Xia et al., 2002), and D898A/D900A eliminates $Ca^{2+}$ sensing via $Ca^{2+}$ bowls (Bao et al., 2004). Before using these mutations, however, it was important to confirm that in conjunction with E399N, they completely eliminate the effect of $Ca^{2+}$ on *Popen*. Shown in Fig. 3 are $Ca^{2+}$ dose–response relations at 0 mV determined from a patch expressing the triple mutant (E399N)(D367A)(D898A/D900A), which we refer to as ΔEΔRΔB, in the presence and absence of β1. As is evident, the triple mutant shows no response to $Ca^{2+}$, which demonstrates that the three sites targeted by these mutations can together account for all $Ca^{2+}$ sensing. Importantly, ΔEΔRΔB + β1 also shows no response to $Ca^{2+}$. Thus, in our hands, β1 does not restore the $Ca^{2+}$ sensitivity of one or more of the sites, as has been suggested (Qian and Magleby, 2003), nor does β1 contain $Ca^{2+}$ binding sites of its own that are coupled to channel opening.

### β1 Alters the Affinity of the $Ca^{2+}$ Bowl Site

We then used the mutant (E399N)(D367A), which we refer to as ΔEΔR, to examine β1's effect on $Ca^{2+}$ sensing at the $Ca^{2+}$ bowl. Fig. 4 displays $BK_{Ca}$ currents from individual patches expressing ΔEΔR in the absence (A) or presence (B) of β1. Each patch was held at 0 mV and exposed to various [$Ca^{2+}$]. For the ΔEΔR channels, application of $Ca^{2+}$ caused an increase in *Popen*, but the increase was not as great (~$10^2$-fold) as it was with the ΔE channel (~$10^5$-fold), likely because the ΔR mutation eliminates half of the channels high-affinity $Ca^{2+}$ binding sites. But more importantly, expression of β1 increased the $Ca^{2+}$ dependence of *Popen* for the ΔEΔR channels. Fig. 4 C shows a comparison of the $Popen/Popen_{min}$ versus [$Ca^{2+}$] relations for the ΔEΔR channel in the presence (filled circles) and absence (open circles) of β1 at 0 mV. Remarkably, for the ΔEΔR channel, the change in *Popen* produced by saturating $Ca^{2+}$ is ~50 times larger in the presence of β1 than it is in its absence. This indicates that β1 increases *C* at the $Ca^{2+}$ bowl site and therefore that it affects $Ca^{2+}$ binding at this site.

To determine the extent to which β1 affects $Ca^{2+}$ binding, in Fig. 4 D, the *Popen* versus [$Ca^{2+}$] relations for the ΔEΔR channels (open circles) and ΔEΔR + β1 channels (filled circles) are plotted. These data are the same as those in Fig. 4 C, except they have been plotted as absolute *Popen*. The affinities of the intact $Ca^{2+}$ bowl site in the presence and absence of β1 were then determined from fits with Eq. 8 below, which is analogous to Eq. 1, but represents the case where there is only one type of $Ca^{2+}$ binding site.

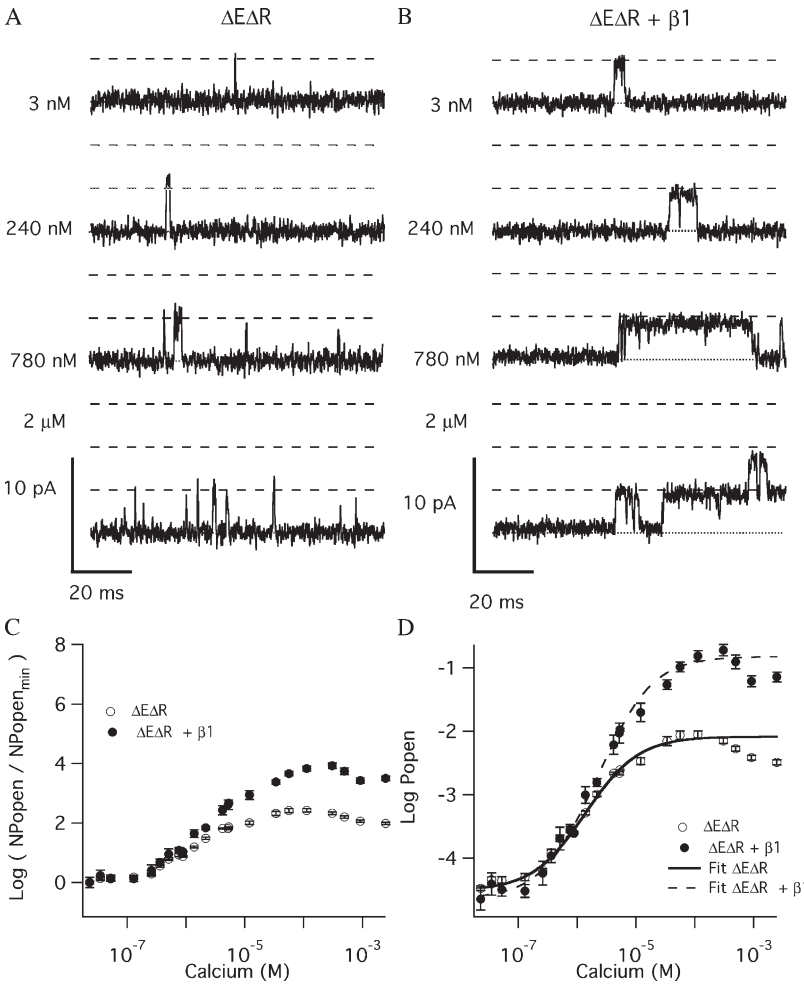


**Figure 4.** β1 alters the affinity of the $Ca^{2+}$ bowl at constant voltage. (A and B) outward $K^+$ currents recorded at 0 mV and filtered at 2 kHz from macropatches containing ΔEΔR channels (A) or ΔEΔR + β1 channels (B) exposed to the indicated [$Ca^{2+}$]. These currents demonstrate that *Popen* increases in a $Ca^{2+}$-dependent manner when voltage is constant. A comparison of the dose–response relation for the effect of $Ca^{2+}$ on *Popen* at 0 mV in the absence or presence of β1 is plotted in C as the ratio of N*Popen* to N$Popen_{min}$ versus [$Ca^{2+}$] and in D as *Popen* versus [$Ca^{2+}$]. Each point represents the average of between 8 and 16 patches at each [$Ca^{2+}$] tested. Error bars represent SEM.

$$Popen = \frac{M(1+[Ca]/K_O)^4}{(1+[Ca]/K_C)^4 + M(1+[Ca]/K_O)^4} \quad (8)$$

Importantly, the bottom of the curve is still determined by *M*, but once *M* is specified, the top of the curve is determined only by *C*. That is, at saturating $Ca^{2+}$,

$$Popen = \frac{1}{1+\frac{1}{M}\left(\frac{1}{C}\right)^4} \quad (9), \quad \text{where} \quad C = \left(\frac{K_C}{K_O}\right) \quad (10).$$

Thus, when there is a single type of binding site, determining the top and bottom of the channel's *Popen* versus [$Ca^{2+}$] curve greatly constrains the fitting. In fact, in leaves only one parameter free, either of the two dissociation constants, to determine the shape of the curve.

Fitting the ΔEΔR channel's *Popen* versus [$Ca^{2+}$] curve yielded the fit shown in Fig. 4 D (solid line). Gratifyingly, even with these constraints the fit closely approximated the data and yielded the following parameters (see also Table I):

$K_C$ = 2.1 ± 0.28 μM, $K_O$ = 0.55 ± 0.08 μM, $C$ = 3.82
$M = 2.8 \times 10^{-6} \pm 5.3 \times 10^{-6}$

Next, we fitted the ΔEΔR + β1 curve (Fig. 4 D, dashed line), and again the fit appeared to well approximate the data. This suggests that β1 does not likely alter the assumptions underlying Eq. 8: a single conformational change between opened and closed; four binding sites; and binding at one site does not affect binding at the other sites, except via promoting opening. The fit yielded the following parameter values:

$K_C$ = 5.9 ± 1.1 μM, $K_O$ = 0.7 ± 0.13 μM, $C$ = 8.4
$M = 2.2 \times 10^{-6} \pm 8.8 \times 10^{-6}$

Note that the fit is well constrained and suggests that β1 reduces the affinity of the $Ca^{2+}$ bowl site for $Ca^{2+}$ both in the opened and the closed channel. The effect on $K_O$ however is smaller than on $K_C$ and not clearly significant. The effect on $K_C$, however, is large (2.8-fold), and it is predominately this change that increases *C* for this site and accounts for the expanded *Popen* range spanned by the ΔEΔR channel's $Ca^{2+}$ dose–response relation in the presence of β1.

Thus, β1 does alter $Ca^{2+}$ binding at the $Ca^{2+}$ bowl site. It lowers the $Ca^{2+}$ bowl's affinity when the channel is closed. Unexpectedly, however, the loss of the channel's

TABLE I

*$Ca^{2+}$ Binding Parameters*

| Binding site | Membrane potential (mV) | $K_C$ (μM) | $K_O$ (μM) | $M \times 10^{-6}$ | C ($K_C/K_O$) |
|---|---|---|---|---|---|
| $Ca^{2+}$ bowl (ΔEΔR) | | | | | |
| α | 0 | 2.1 ± 0.28 | 0.55 ± 0.08 | 2.8 ± 5.3 | 3.8 |
| α+β1 | 0 | 5.9 ± 1.1 | 0.70 ± 0.13 | 2.2 ± 8.8 | 8.4 |
| RCK1 (ΔEΔB) | | | | | |
| α | 0 | 15.8 ± 3.1 | 2.10 ± 0.40 | 18 ± 4.5 | 7.5 |
| α+β1 | 0 | 18.5 ± 4.4 | 0.52 ± 0.07 | 0.15 ± 0.05 | 36 |

RCK1 sites also had a dramatic effect on β1's influence on the $Ca^{2+}$-independent properties of channel gating. The β1-induced change in *M*, which was 235-fold for the ΔE channel (Fig. 2 D), is absent in ΔEΔR channel. Indeed, with the D367A mutation present, it appears β1 no longer effects *M*. The bottoms of the two curves in Fig. 2 D are at the same place on the log (*Popen)* axis. This result argues that functional RCK1 sites are required for β1's effect on the intrinsic equilibrium constant between open and closed, usually referred to as *L* (for an analysis of mouse β1's effects on *L* see Wang and Brenner 2006).

### β1 also Alters the Affinities of the RCK1 Sites

To examine β1's effect on $Ca^{2+}$ sensing at the RCK1 sites we used the mutant (E399N) (D898A/D900A), which we refer to as ΔEΔB. In Fig. 5, $BK_{Ca}$ currents from individual patches expressing ΔEΔB channels in the absence (A) or presence of β1 (B) are displayed. Patches were held at 0 mV and exposed to various [$Ca^{2+}$]. For ΔEΔB channels application of $Ca^{2+}$ caused an increase in *Popen*, but again the increase is not as great (~$10^4$-fold) as it is with the ΔE channel (~$10^5$-fold), presumably because the ΔEΔB channel had lost half of its high-affinity $Ca^{2+}$ binding sites. More importantly, however, coexpression of β1 increased the maximal effect of $Ca^{2+}$ on *Popen*. Fig. 5 C shows a comparison of the $Popen/Popen_{min}$ versus [$Ca^{2+}$] relations for the ΔEΔB channel in the presence (filled circles) and absence (open circles) of β1. The effect of β1 on $Ca^{2+}$ sensing via the RCK1 sites is substantial. For the ΔEΔB channel, the change in *Popen* produced by saturating $Ca^{2+}$ is ~400 times larger in the presence of the β1. This again requires that β1 increase *C* ($K_{C1}/K_{O1}$) at the RCK1 site and therefore that it affects $Ca^{2+}$ binding at this site as well.

To determine how much each dissociation constant is affected, we plotted (Fig. 5 D) the *Popen* versus [$Ca^{2+}$] relations for the ΔEΔB (open circles) and ΔEΔB + β1 (filled circles) channels and fit these relations with Eq. 8. The affinities of the intact RCK1 sites in the presence and absence of β1 were then determined from the fits. The fit to the ΔEΔB data (solid line) yielded the following values (see also Table I):

$$K_C = 15.8 \pm 3.1\ \mu M,\ K_O = 2.1 \pm 0.43\ \mu M,\ C = 7.5$$
$$M = 1.8 \times 10^{-5} \pm 0.45 \times 10^{-5}$$

And the fit to the ΔEΔB + β1 data (dashed curve) yielded the following values (see also Table I):

$$K_C = 18.5 \pm 4.4\ \mu M,\ K_O = 0.52 \pm 0.07\ \mu M,\ C = 36$$
$$M = 1.5 \times 10^{-7} \pm 0.5 \times 10^{-7}$$

Thus, there is a small β1-induced change in the affinity of the RCK1 sites when the channel is closed, and a much larger relative change when the channel is open, the opposite of what we observed at the $Ca^{2+}$ bowl. Most important, however, the changes are diametric and consequently the change in *C* is large (7.5→36), and it is this change that drives the expansion of the channel's $Ca^{2+}$ dose–response curve along the ordinate in Fig. 5 C upon β1 coexpression. Interestingly, the β1-induced change in *M* is ~200-fold for the ΔEΔB channel, similar to what is observed with the ΔE channel. Thus, unlike functional RCK1 sites, functional $Ca^{2+}$ bowls are not required for β1's effects on the $Ca^{2+}$-independent gating properties of the $BK_{Ca}$ channel.

Although β1 has very large effects on the ΔEΔB channel's $Ca^{2+}$ dose–response relation, there is a complicating factor that makes our conclusions about the effects of β1 on this site less than definitive. Our analysis assumes that there are no direct interactions between $Ca^{2+}$ binding sites and voltage sensors. We have however shown previously (Sweet and Cox, 2008) that $Ca^{2+}$ binding at the RCK1 site is voltage dependent, an effect that is most reasonably attributed to a direct intrasubunit interaction between voltage sensor and RCK1 $Ca^{2+}$ binding site. Further, we have estimated the allosteric factor by which voltage sensor activation alters the equilibrium constant for $Ca^{2+}$ binding at the RCK1 site (*E*) to be ~2.8, and Horrigan and Aldrich (2002) arrived at a similar value, 2.4, based on the effect of $Ca^{2+}$ on voltage sensor movement measured with gating currents. This means that Eq. 8 is not strictly correct for the ΔEΔB channel because as $Ca^{2+}$ binds and the channels open, more voltage sensors will become active, even if the voltage is held constant, and this could lead to enhanced binding not accounted for by Eq. 8. The magnitude of this effect will depend on *E* and on the properties of the channel's voltage sensors. In terms of the Horrigan and Aldrich (HA) model, it will depend on *L* and $V_{hc}$, and $V_{ho}$, $z_L$, and $z_J$ (Horrigan and Aldrich, 2002). Furthermore, if β1 changes any of these

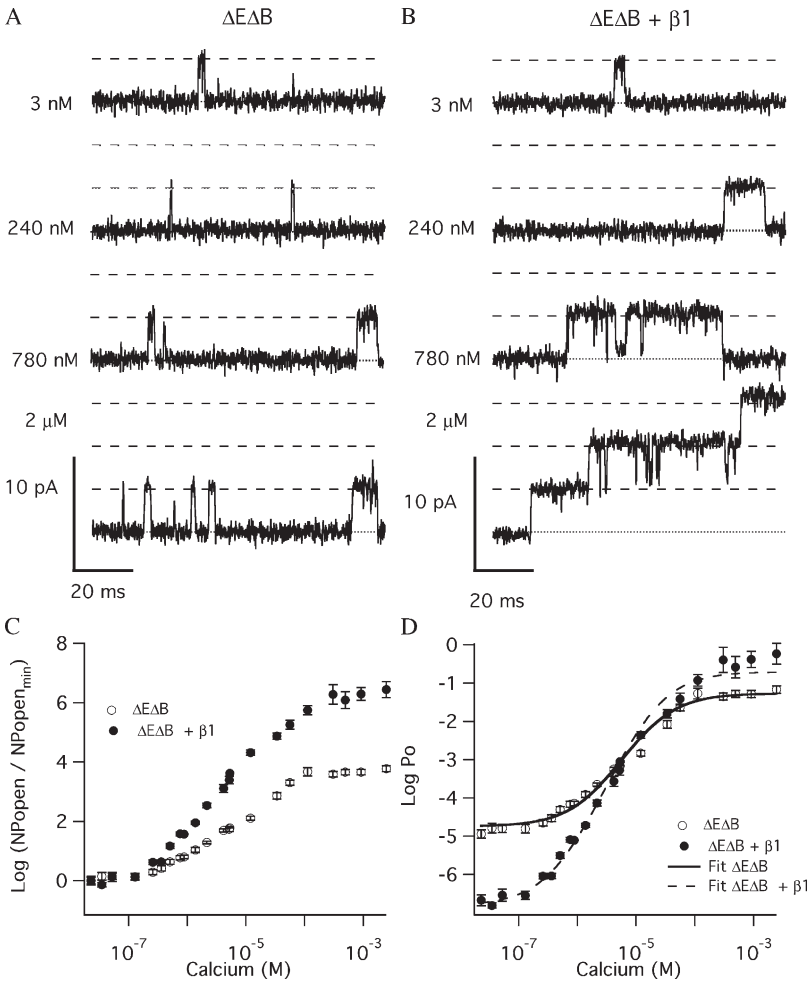


**Figure 5.** β1 alters the affinity of the RCK1 site at constant voltage. (A and B) Outward $K^+$ currents recorded at 0 mV and filtered at 2 kHz from macropatches containing ΔEΔB channels (A) or ΔEΔB + β1 channels (B) exposed to the indicated [$Ca^{2+}$]. These currents demonstrate that *Popen* increases in a $Ca^{2+}$-dependent manner when voltage is constant. A comparison of the dose–response relation for the effect of $Ca^{2+}$ on *Popen* at 0 mV in the absence or presence of β1 is shown in C as the ratio N*Popen* to N$Popen_{min}$ versus [$Ca^{2+}$] and in D as *Popen* versus [$Ca^{2+}$]. Each point represents the average of between 5 and 22 patches at each [$Ca^{2+}$] tested. Error bars represent SEM.

parameters this could alter the channel's $Ca^{2+}$ dose–response curve in a way that looks like an increase in *C*, when no real change in *C* has occurred.

Ideally, our experiments would have been performed at a negative voltage where the channel's voltage sensors are very rarely active; however, in the presence of the β1 subunit voltage sensors become active at far negative voltages where *Popen* at 3 nM [$Ca^{2+}$] is too low to measure well, making this approach impractical. However, we examined whether the effects of β1 on the $BK_{Ca}$ channel's voltage sensing parameters could account for its effects on the ΔEΔB channel's *Popen* versus [$Ca^{2+}$] curve as follows. We simulated ΔEΔB *Popen* versus [$Ca^{2+}$] curves using the HA model and voltage-sensing parameters that have been well established for the wild-type mSlo1 channel ($V_{ho}$ = 27 mV, $V_{hc}$ = 151 mV, $z_J$ = 0.58, $z_L$ = 0.41, $L0 = 2 \times 10^{-6}$, and $E$ = 2.8) and $Ca^{2+}$ dissociation constants we determined for the RCK1 site ($K_C$ = 23.2 μM and $K_O$ = 4.9 μM). This led to the *Popen* versus [$Ca^{2+}$] curve shown in Fig. 6 B (dark curve). We then simulated the effects of β1 on the voltage-sensing parameters of the channel by lowering *L* from $2 \times 10^{-6}$ to $2 \times 10^{-9}$ to account for the large decline in *M* (*Popen* at 3 nM $Ca^{2+}$), and we altered $V_{hc}$ to +80 mV and $V_{ho}$ to −34 mV, parameters we have determined previously for α+β1 channels (Bao and Cox, 2005). The resulting curve is also shown in Fig. 6 B (gray curve), and as anticipated, altering these voltage-sensing parameters did increase the maximum effect of $Ca^{2+}$ on *Popen*. The change in *Popen* brought about by saturating [$Ca^{2+}$] increased 1.55-fold. Thus, some of the changes we have observed in the ΔEΔB channel's *Popen* versus [$Ca^{2+}$] curve upon β1 expression likely arise from β1's effects on voltage sensing rather than $Ca^{2+}$ binding. However, as seen in Fig. 6 A, β1 increases the maximum effect of $Ca^{2+}$ on *Popen* 708-fold—far greater than the effect we anticipate due to the linkage between $Ca^{2+}$ binding and voltage sensing (1.55-fold). In fact the anticipated effect is <1% of the true effect of β1. Thus, this complication not withstanding, it does appear that β1 alters the true $Ca^{2+}$ affinities of the RCK1 sites as well as the $Ca^{2+}$ bowl sites.

## DISCUSSION

Here, we have examined the mechanism by which the $BK_{Ca}$ channel's β1 subunit increases the $Ca^{2+}$ sensitivity of channel activation. To be as accurate as possible, we used unitary–current recordings from patches containing from a few hundred to just a few channels. This

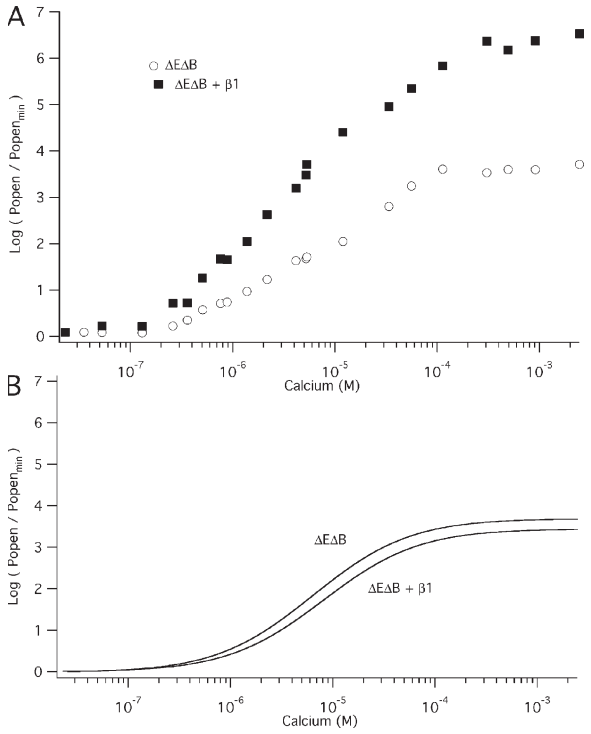


**Figure 6.** β1's effects on the $BK_{Ca}$ channel's voltage-sensing parameters cannot account for the β1-induced changes in the ΔEΔB channel's $Ca^{2+}$ dose–response relation. (A) ΔEΔB (open circles) and ΔEΔB + β1 (filled squares) $Ca^{2+}$ dose–response relations normalized to their minima. (B) Simulated $Ca^{2+}$ dose–response curves for the ΔEΔB (black curve) and ΔEΔB + β1 (gray curve) channels assuming that β1 only affects the voltage-sensing properties of the channel. The curves were simulated with an HA model using parameters we have determined previously (Bao and Cox, 2005; Sweet and Cox, 2008). For the ΔEΔB (α-only channel): *L* = 2e-6, Vhc =151 mV, Vho = 27 mV, E = 2.8, and zL = 0.41, and zJ = 0.58, Kc = 23.2 μM, and Ko = 4.9 μM. To simulate the effects of β1, L0 was moved to 2e-9, Vhc to 80 mV, and Vho to −34 mV. The remaining parameters were unchanged.

allowed us to determine *Popen* over seven orders of magnitude. To be as model independent as possible, we made measurements at constant voltage, and where possible low *Popen*, such that the amplitudes and shapes of the resulting $Ca^{2+}$ dose–response curves were dependent primarily, if not exclusively, on the channel's $Ca^{2+}$ binding parameters. The essential assumptions we made in fitting our data were as follows: (1) that there is a single conformational change between open and closed that can occur with any number of $Ca^{2+}$ bound, an idea that is consistent with a great many single-channel and macroscopic $BK_{Ca}$ channel studies and all current models (McManus and Magleby, 1991; Cox et al., 1997; Cui et al., 1997; Horrigan et al., 1999; Horrigan and Aldrich, 1999, 2002; Rothberg and Magleby, 1999, 2000; Cox and Aldrich, 2000a); (2) that there are four of each type of high-affinity site. This has been established for the $Ca^{2+}$ bowl (Niu and Magleby, 2002), and given the fourfold symmetry of the channel, this seems likely to be the case for the RCK1 site as well; and (3) that there are no interactions between binding sites of the same type or between $Ca^{2+}$ binding and voltage sensor movement.

We found that the 0 mV $Ca^{2+}$ dose–response curve of $BK_{Ca}$ channels containing only functional RCK1 sites could be well fitted by supposing that each site independently influences opening, and that each site has a dissociation constant of 15.8 μM when the channel is closed and 2.1 μM when the channel is open. These values produce a *C* value of 7.5, which allows us to calculate that each $Ca^{2+}$ bound to a $Ca^{2+}$ bowl site decreases the energy difference between open and closed by 4.9 KJ/mol.

In the presence of β1, the RCK1 site's dose–response curve at 0 mV could also be well fitted with a simple model and yielded values for $K_C$ and $K_O$ of 18.5 and 0.52 μM, respectively. These values produce a substantial *C* value of 36 (8.8 KJ/mol per binding event), which we think is in large part responsible for the dramatic increase in the influence of $Ca^{2+}$ on *Popen* brought about by β1 in the ΔEΔB channels. As discussed above, however, our estimates of these values are complicated by an interaction between $Ca^{2+}$ binding and voltage at the RCK1 sites. But we have simulated the influence that this complication will likely have on $Ca^{2+}$ binding in the presence of β1, and it turns out to very small compared with the effect of β1 observed. Thus, we do not think this linkage has greatly distorted our measurement of $K_C$ and $K_O$.

$Ca^{2+}$ binding to the $Ca^{2+}$ bowl is not voltage sensitive (Sweet and Cox, 2008); thus, our conclusions drawn from data for the $Ca^{2+}$ bowl sites are more clear. We found that the $Ca^{2+}$ bowl's dose–response curve at 0 mV could be well fitted by supposing that each $Ca^{2+}$ bowl independently influences opening, and that each site has a dissociation constant for $Ca^{2+}$ of 2.1 μM when the channel is closed and 0.56 μM when the channel is open. These values produce a *C* of 3.75, which allows us to calculate that each $Ca^{2+}$ bound at a $Ca^{2+}$ bowl site decreases the energy difference between open and closed by 3.2 KJ/mol. These numbers may be compared with previous estimates of $K_C$ and $K_O$ for this site. Xia et al. (2002) estimated $K_C = 4.5 \pm 1.7$ μM and $K_O = 2.0 \pm 0.7$ μM (C = 2.25), and Bao et al. (2002) estimated $K_C = 3.8 \pm 0.2$ and $K_O = 0.94 \pm 0.06$ μM ($C = 4.0$). And in Sweet and Cox (2008), we estimated $K_C = 3.13 \pm 0.28$ μM and $K_O = 0.88 \pm 0.06$ μM ($C = 3.55$). Thus, our current estimates are close to our previous estimates, especially in terms of *C*.

More interestingly, we found that coexpression of β1 changed the ΔEΔR channel's *Popen* versus [$Ca^{2+}$] relation in a manner that indicated that the affinity of the $Ca^{2+}$ bowl site for $Ca^{2+}$ is changed in the presence of β1. In the presence of β1, the ΔEΔR channel's dose–response curve at 0 mV could be well fitted by supposing that each $Ca^{2+}$ bowl independently influences opening, and that each site has an affinity of 5.9 μM when the channel is closed and 0.67 μM when the channel is open. These values produce a *C* value of 8.8, which allows us to calculate that with β1

present, each $Ca^{2+}$ bound at a $Ca^{2+}$ bowl decreases the energy difference between open and closed by 5.3 KJ/mol.

These numbers are difficult to compare with previous estimates of the affinities of the $BK_{Ca}$ channel in the presence of β1. Bao and Cox (2005) estimated the affinities of the channel in the presence of β1 to be $K_C$ = 3.71 μM and $K_O$ = 0.88 μM ($C$ = 4.2) for site 1 and $K_C$ = 5.78 μM and $K_O$ = 0.73 μM ($C$ = 7.9) for site 2. These estimates, however, were based on the assumption that β1 affected the affinity of only one of the two binding sites (site 2), which we now think is not the case. But interestingly, and of relevance here, Cox and Aldrich (2000) observed that the affinity of the channel for $Ca^{2+}$ in the open conformation must not change upon expression of β1, as β1 does not alter the critical [$Ca^{2+}$] required to begin to see a leftward shift in the channel's G-V relation (Cox and Aldrich, 2000a). This is in agreement with our data that show that expression of β1 does not appreciably alter $K_O$ for the higher-affinity site ($Ca^{2+}$ bowl: $Ko_{\alpha}$ = 0.56 μM, $K_{O\alpha+\beta 1}$ = 0.67 μM).

In considering the effects of β1 on $Ca^{2+}$ binding, it is interesting to note that the $BK_{Ca}$ β1 subunit has very little intracellular sequence, just its N and C termini—15 and 13 amino acids long, respectively. The rest of the protein is comprised of two transmembrane domains and a large extracellular loop—118 amino acids. Thus, if β1 subunits alter the channel's affinity for $Ca^{2+}$ by interacting directly with $Ca^{2+}$ binding sites, generally accepted to be contained within the cytoplasmic C terminus of the channel, they seemingly must do so through these short intracellular termini. Supporting this idea, chimera experiments with β1 and β2 (Orio and Latorre, 2005) and β1 N- and C-terminal deletion experiments (Wang and Brenner, 2006) have shown that these termini play a critical role in transmitting β1's effects to the channel proper.

In addition to β1's effects on $Ca^{2+}$ binding, and in agreement with the previous findings of Wang and Brenner (2006), we found that mouse β1 reduces *Popen* at 0 mV in the absence of $Ca^{2+}$, presumably by lowering *L*. Strikingly, our results show that a mutation at a $Ca^{2+}$ binding site (D367A) not only eliminates $Ca^{2+}$ binding at the RCK1 sites, but it also eliminates β1's ability to reduce *Popen* at 0 mV in the absence of $Ca^{2+}$. That is, a single $Ca^{2+}$ binding site mutation affects both the mechanism by which the channel senses $Ca^{2+}$ and also the mechanism by which β1 influences the intrinsic energetics of opening.

We also found that when we combine mutations at all three types of $Ca^{2+}$ binding sites—E399N (low-affinity site), D367A (RCK1 site), and D898/D900 ($Ca^{2+}$ bowl)—we see no effect of $Ca^{2+}$ on channel gating in the α-only channel, and we see no restoration of an effect of $Ca^{2+}$ on channel gating by β1. This in contrast to the work of Qian and Magleby (2003), who found that coexpression of β1 restored some $Ca^{2+}$ sensitivity to a similar triple mutant. We do not know why we did not see the restorative effect of β1 observed by Qian and Magleby. The most straightforward explanation is that the $Ca^{2+}$ binding sites were disabled by the mutations and could not be fixed by β1. However, the main differences between the two studies were as follows: our recordings were made at 0 mV, whereas theirs were conducted at +50 mV. The mutations used at each binding site were not exactly the same between the two studies, and Qian and Magleby recorded from single-channel patches, whereas the patches we used typically contained many channels. Furthermore, Qian and Magleby did not see the restorative effect of β1 in every experiment, but rather they reported a large variability from patch to patch. This would seem to suggest that perhaps there is a subtle environmental factor required for the effect they observed that was absent from our experiments.

Our measurements of the effects of β1 on $Ca^{2+}$ binding also stand in some contrast to the recent paper of Yang et al. (2008). They found that the mutation R167A in the voltage-sensing domain of the mSlo1 channel eliminates β1's ability to alter the channel's G-V curve at all [$Ca^{2+}$]. This result suggests that by altering just voltage sensor movement one can disrupt the β1-induced enhancement of $Ca^{2+}$ sensitivity altogether. It seems hard to imagine how such a mutation could simultaneously eliminate β1's effects on voltage sensor movement and $Ca^{2+}$ binding at both binding sites, unless these processes are physically more intertwined than previously thought.

Perhaps rather than affecting $Ca^{2+}$ binding directly, the β1 subunit might be affecting a linkage between $Ca^{2+}$ binding and voltage sensing, which in turn affects $Ca^{2+}$ binding. Indeed, we have shown recently (Sweet and Cox, 2008) that such a linkage exists between the RCK1 sites and the voltage sensors, so it is possible that an enhancement of the allosteric factor at this linkage, *E*, could create enhanced binding affinity. It would be interesting to explore this linkage in α+β1 channels. However, we found no such linkage between $Ca^{2+}$ bowl sites and the channel's voltage sensors (Sweet and Cox, 2008); thus, we do not think that such an effect is involved in the β1-induced changes in the binding affinity we observed at the $Ca^{2+}$ bowl sites.

In conclusion, we have shown that the BK β1 subunit has effects on the affinities of the $BK_{Ca}$ channel's high-affinity $Ca^{2+}$ binding sites. It primarily increases the affinity of the RCK1 sites when the channel is open, and it primarily decreases the affinity of the $Ca^{2+}$ bowl sites when the channel is closed. Both of these modifications increase the difference in affinity between open and closed, such that $Ca^{2+}$ binding at either site has a larger effect on channel opening when β1 is present.

This work was supported by program project grant P01-HL077378 and predoctoral fellowship F31 NS047823 from the National Institutes of Health.

Edward N. Pugh Jr. served as editor.

Submitted: 1 October 2008
Accepted: 18 December 2008

## REFERENCES


Bao, L., and D.H. Cox. 2005. Gating and ionic currents reveal how the $BK_{Ca}$ channel's $Ca^{2+}$ sensitivity is enhanced by its β1 subunit. *J. Gen. Physiol.* 126:393–412.

Bao, L., A.M. Rapin, E.C. Holmstrand, and D.H. Cox. 2002. Elimination of the $BK_{Ca}$ channel's high-affinity $Ca^{2+}$ sensitivity. *J. Gen. Physiol.* 120:173–189.

Bao, L., C. Kaldany, E.C. Holmstrand, and D.H. Cox. 2004. Mapping the $BK_{Ca}$ channel's "$Ca^{2+}$ bowl": side-chains essential for $Ca^{2+}$ sensing. *J. Gen. Physiol.* 123:475–489.

Bian, S., I. Favre, and E. Moczydlowski. 2001. Ca2+-binding activity of a COOH-terminal fragment of the Drosophila BK channel involved in Ca2+-dependent activation. *Proc. Natl. Acad. Sci. USA.* 98:4776–4781.

Brenner, R., G.J. Perez, A.D. Bonev, D.M. Eckman, J.C. Kosek, S.W. Wiler, A.J. Patterson, M.T. Nelson, and R.W. Aldrich. 2000. Vasoregulation by the beta1 subunit of the calcium-activated potassium channel. *Nature.* 407:870–876.

Butler, A., S. Tsunoda, D.P. McCobb, A. Wei, and L. Salkoff. 1993. mSlo, a complex mouse gene encoding "maxi" calcium-activated potassium channels. *Science.* 261:221–224.

Cox, D.H., and R.W. Aldrich. 2000. Role of the β1 subunit in large-conductance $Ca^{2+}$-activated $K^+$ channel gating energetics. Mechanisms of enhanced $Ca^{2+}$ sensitivity. *J. Gen. Physiol.* 116:411–432.

Cox, D.H., J. Cui, and R.W. Aldrich. 1997. Allosteric gating of a large conductance Ca-activated $K^+$ channel. *J. Gen. Physiol.* 110:257–281.

Cui, J., D.H. Cox, and R.W. Aldrich. 1997. Intrinsic voltage dependence and $Ca^{2+}$ regulation of *mslo* large conductance Ca-activated $K^+$ channels. *J. Gen. Physiol.* 109:647–673.

Hamill, O.P., A. Marty, E. Neher, B. Sakmann, and F.J. Sigworth. 1981. Improved patch-clamp techniques for high-resolution current recording from cells and cell-free membrane patches. *Pflugers Arch.* 391:85–100.

Horrigan, F.T., and R.W. Aldrich. 1999. Allosteric voltage gating of potassium channels II; mSlo channel gating charge movement in the absence of $Ca^{2+}$. *J. Gen. Physiol.* 114:305–336.

Horrigan, F.T., and R.W. Aldrich. 2002. Coupling between voltage sensor activation, $Ca^{2+}$ binding and channel opening in large conductance (BK) potassium channels. *J. Gen. Physiol.* 120:267–305.

Horrigan, F.T., J. Cui, and R.W. Aldrich. 1999. Allosteric voltage gating of potassium channels I: mSlo ionic currents in the absence of $Ca^{2+}$. *J. Gen. Physiol.* 114:277–304.

McManus, O.B., and K.L. Magleby. 1991. Accounting for the Ca(2+)-dependent kinetics of single large- conductance Ca(2+)-activated K+ channels in rat skeletal muscle. *J. Physiol.* 443:739–777.

McManus, O.B., L.M. Helms, L. Pallanck, B. Ganetzky, R. Swanson, and R.J. Leonard. 1995. Functional role of the beta subunit of high conductance calcium-activated potassium channels. *Neuron.* 14:645–650.

Meera, P., M. Wallner, Z. Jiang, and L. Toro. 1996. A calcium switch for the functional coupling between alpha (hslo) and beta subunits (KV,Ca beta) of maxi K channels. *FEBS Lett.* 382:84–88.

Morrow, J.P., S.I. Zakharov, G. Liu, L. Yang, A.J. Sok, and S.O. Marx. 2006. Defining the BK channel domains required for beta1-subunit modulation. *Proc. Natl. Acad. Sci. USA.* 103:5096–5101.

Nelson, M.T., and J.M. Quayle. 1995. Physiological roles and properties of potassium channels in arterial smooth muscle. *Am. J. Physiol.* 268:C799–C822.

Nelson, M.T., H. Cheng, M. Rubart, L.F. Santana, A.D. Bonev, H.J. Knot, and W.J. Lederer. 1995. Relaxation of arterial smooth muscle by calcium sparks. *Science.* 270:633–637.

Nimigean, C.M., and K.L. Magleby. 1999a. β subunits increase the calcium sensitivity of mSlo by stabilizing bursting kinetics. *Biophys. J.* 76:A328.

Nimigean, C.M., and K.L. Magleby. 1999b. The β subunit increases the $Ca^{2+}$ sensitivity of large conductance $Ca^{2+}$-activated potassium channels by retaining the gating in the bursting states. *J. Gen. Physiol.* 113:425–440.

Nimigean, C.M., and K.L. Magleby. 2000. Functional coupling of the $\beta_1$ subunit to the large conductance $Ca^{2+}$-activated $K^+$ channel in the absence of $Ca^{2+}$. Increased $Ca^{2+}$ sensitivity from a $Ca^{2+}$-independent mechanism. *J. Gen. Physiol.* 115:719–736.

Niu, X., and K.L. Magleby. 2002. Stepwise contribution of each subunit to the cooperative activation of BK channels by Ca2+. *Proc. Natl. Acad. Sci. USA.* 99:11441–11446.

Orio, P., and R. Latorre. 2005. Differential effects of β1 and β2 subunits on BK channel activity. *J. Gen. Physiol.* 125:395–411.

Orio, P., Y. Torres, P. Rojas, I. Carvacho, M.L. Garcia, L. Toro, M.A. Valverde, and R. Latorre. 2006. Structural determinants for functional coupling between the β and α subunits in the $Ca^{2+}$-activated $K^+$ (BK) channel. *J. Gen. Physiol.* 127:191–204.

Perez, G.J., A.D. Bonev, J.B. Patlak, and M.T. Nelson. 1999. Functional coupling of ryanodine receptors to KCa channels in smooth muscle cells from rat cerebral arteries. *J. Gen. Physiol.* 113:229–238.

Pluger, S., J. Faulhaber, M. Furstenau, M. Lohn, R. Waldschutz, M. Gollasch, H. Haller, F.C. Luft, H. Ehmke, and O. Pongs. 2000. Mice with disrupted BK channel beta1 subunit gene feature abnormal Ca(2+) spark/STOC coupling and elevated blood pressure. *Circ. Res.* 87:E53–E60.

Qian, X., and K.L. Magleby. 2003. Beta1 subunits facilitate gating of BK channels by acting through the Ca2+, but not the Mg2+, activating mechanisms. *Proc. Natl. Acad. Sci. USA.* 100:10061–10066.

Qian, X., C.M. Nimigean, X. Niu, B.L. Moss, and K.L. Magleby. 2002. Slo1 tail domains, but not the $Ca^{2+}$ bowl, are required for the β1 subunit to increase the apparent $Ca^{2+}$ sensitivity of BK channels. *J. Gen. Physiol.* 120:829–843.

Rothberg, B.S., and K.L. Magleby. 1999. Gating kinetics of single large-conductance $Ca^{2+}$-activated $K^+$ channels in high $Ca^{2+}$ suggest a two-tiered allosteric gating mechanism. *J. Gen. Physiol.* 114: 93–124 (published erratum in 114:337).

Rothberg, B.S., and K.L. Magleby. 2000. Voltage and $Ca^{2+}$ activation of single large-conductance $Ca^{2+}$-activated $K^+$ channels described by a two-tiered allosteric gating mechanism. *J. Gen. Physiol.* 116:75–99.

Schreiber, M., and L. Salkoff. 1997. A novel calcium-sensing domain in the BK channel. *Biophys. J.* 73:1355–1363.

Shen, K.Z., A. Lagrutta, N.W. Davies, N.B. Standen, J.P. Adelman, and R.A. North. 1994. Tetraethylammonium block of Slowpoke calcium-activated potassium channels expressed in Xenopus oocytes: evidence for tetrameric channel formation. *Pflugers Arch.* 426:440–445.

Shi, J., G. Krishnamoorthy, Y. Yang, L. Hu, N. Chaturvedi, D. Harilal, J. Qin, and J. Cui. 2002. Mechanism of magnesium activation of calcium-activated potassium channels. *Nature.* 418:876–880.

Sweet, T.B., and D.H. Cox. 2008. Measurements of the $BK_{Ca}$ channel's high-affinity $Ca^{2+}$ binding constants: effects of membrane voltage. *J. Gen. Physiol.* 132:491–505.

Wallner, M., P. Meera, and L. Toro. 1996. Determinant for beta-subunit regulation in high-conductance voltage-activated and Ca(2+)-sensitive K+ channels: an additional transmembrane region at the N terminus. *Proc. Natl. Acad. Sci. USA.* 93:14922–14927.

Wang, B., and R. Brenner. 2006. An S6 mutation in BK channels reveals β1 subunit effects on intrinsic and voltage-dependent gating. *J. Gen. Physiol.* 128:731–744.

Xia, X.M., X. Zeng, and C.J. Lingle. 2002. Multiple regulatory sites in large-conductance calcium-activated potassium channels. *Nature.* 418:880–884.

Yang, H., G. Zhang, J. Shi, U.S. Lee, K. Delaloye, and J. Cui. 2008. Subunit-specific effect of the voltage sensor domain on Ca2+ sensitivity of BK channels. *Biophys. J.* 94:4678–4687.

Yang, X.C., and F. Sachs. 1989. Block of stretch-activated ion channels in Xenopus oocytes by gadolinium and calcium ions. *Science.* 243:1068–1071.